Journal of Mines, Metals and Fuels, *71(12): 2708-2717; 2023. DOI: 10.18311/jmmf/2023/41762*

Print ISSN : 0022-2755

Journal of Mines, Metals and Fuels

Contents available at: *www.informaticsjournals.com/index.php/jmmf*

Characteristic Analysis of Soret and Corolis Forces on a Natural Convection in a Finite Cavity with Isotropic and Anisotropic Permeable Media

Sudhir Patel[1]*, P. A. Dinesh[2], S. P. Suma[3], T. C. Sushma[4] and M. S. Gayathri[5]

[1]*Department of Mathematics, New Horizon College of Engineering, Bangalore – 560103, Karnataka India; sudhirp@newhorizonindia.edu*
[2]*Department of Mathematics, Ramaiah Institute of Technology, Bangalore – 560054, Karnataka, India*
[3]*Department of Mathematics, Cambridge Institute of Technology, Bangalore – 560036, Karnataka, India*
[4]*Department of Mathematics, Nitte Meenakshi Institute of Technology, Bangalore – 560 064, Karnataka, India*
[5]*Department of Mathematics, B. M. S College of Engineering, Bangalore – 560 019, Karnataka, India*

Abstract

Using 3D transmission in a definite cavity with anisotropic and isotropic permeable media rotating at a fixed rotational velocity, the Rayleigh-Benard issue for a viscous, unstable, laminar, incompressible fluid heated from below a horizontal layer is extended in this paper's research. Seven controlling PDEs from the given physical configuration are similarly transformed to produce a system of non-dimensional ODEs. The Rayleigh, Taylor, and Prandtl numbers are examined for their impacts on temperature gradient and velocity in both isotropic and anisotropic conditions using the Fourier series approach. It has been discussed and determined that the results of the stream function and isotherms on a variety of factors are good.

Keywords: *Anisotropic Porous Media, Coriolis force, Isotropic, Natural Convection, Soret Effect*

1.0 Introduction

Due to its numerous important technical and geophysical applications, such as chemical catalytic reactors and nuclear waste dumps, thermal convection in a fluid-saturated porous medium has attracted a lot of attention recently. Nield and Bejan[1] and Ingham and Pop[2] have all done a lot of study on this topic. The Soret effect, a second-order fluid phenomenon, becomes an important feature when the concentration and temperature gradients are appreciably considerable.

The importance of the Soret effect in gas mixtures with low and medium molecular masses as well as the diffusion of matter brought on by temperature gradients are covered by Eckert and Drake[3]. The Soret effect was investigated by Rudriah and Patil[4], although their conclusions were limited to open borders.

A magnetic field's impact on a Darcy–free convection of mass and heat from vertical surfaces have been studied by Postelnicu[6]. The impact of this phenomena on free convection flow was studied by Anghel *et al*. Partha *et al.*[7] studied the effects of Soret on non-Darcy porous media thermal convection from a vertical plate using an electrically conducting saturated fluid; both heat and solvent dispersion in the medium were taken into consideration.

The Soret effect on a Darcy porous media in free convection heat and mass transport from a horizontal flat plate was studied by Lakshmi Narayana and Murthy[8], Mansour *et al.*,[9] studied the Soret effect in a square porous

*Author for correspondence

cavity heated from below and subjected to a horizontal concentration gradient in order to evaluate the diversity of solutions caused by thermosolutal convection. Lakshmi Narayana and associates investigated the Soret effect in a doubly organised horizontal stratum. porous spongy media[10].

Due to their importance in numerous industrial applications, natural convection and chemical reactions have also recently garnered a great deal of attention[11]. Investigated the development of chemicals on thermal convection in a suction and injection-driven non-linear MHD laminar boundary layer flow across a wedge.

Due to its use in isotope separation and in a combination of gases with light molecular weight, the Soret effect is prominent in fluids with extremely light and medium weighted molecules[12]. According to Alam *et al.*, work's on Soret effects in mixed convective heat and mass transfer flow across a semi-infinite vertical porous plate[13], the soret effect is important for fluids of medium molecular mass and shouldn't be disregarded.

The Soret effect has a significant impact on the flow field, according to Srinivasacharya and RamReddy's[14] examination of a boundary layer study for mixed convection over a vertical plate with homogeneous mass and heat flux conditions in a non-Darcy micropolar fluid.

In a pair stress liquid layer with linearity and non-linearity of double diffusive convection[15] investigated the Soret effect. Through their research, they learned that a soret number greater than zero stabilises the system whereas a soret number less than zero leads to instability.

The mantle's precessional motion causes the fluid core to rotate on the axis other than mantle. The basic solid body rotation is altered by the differential rotation of the core and mantle, resulting in the appearance of internal shear layers and jets. Precession and tides both have the potential to cause instability in the solution, in this fluid particles in a rotational motion follow streamlines elliptically with the previously mentioned weak shear zones superimposed. This instability would result in smaller eddies and velocity field which is more complex[16].

The primary goal of the work presented is to determine what changes in characteristics will occur when external coriolies force and soret effect are taken into account when studying natural convection in a definite geometry loaded with porous medium which is anisotropic or isotropic. To our knowledge, there is no mention of such a study in the literature mentioned above. The use of science and technology is addressed in a number of real-world scenarios, though call for a knowledge of the Soret effect in a rotational physical system that is crucial to the industrial arena. The detailed governing equations and accompanying Boundary Conditions (BCs) of the physical setup are obtained in the next sections. Later, We use Fourier series analysis to invoke the solution and comprehend the properties of velocity, temperature, and concentration. The final portion focuses on numerically computing the solution and analysing the physical problem's outcomes in relation to various non-dimensional problem parameters.

2.0 Mathematical Formulation

Consideration is given to a non-uniformly heated free convection in three dimensions inside a rectangular porous box. A homogeneous, incompressible fluid is thought to have saturated and an-isotropic effects on the porous medium. The box is rectangular and has measurements of a and h. The vertical direction is chosen as the z-axis, the horizontal box length is chosen as the x axis, and the walls of the rectangular cavity are positioned at z = (0,h). When using the Boussinesq approximation and ignoring inertia considerations, Prandtl-Darcy number is thought to be extraordinarily large. The Darcy-Boussinesq equations' 3-D model has the following form:

$$\frac{\partial u}{\partial x}+\frac{\partial u}{\partial z}=0, \tag{2.1}$$

$$\frac{1}{\rho_0}\frac{\partial p}{\partial y}+\frac{v}{k_y}\upsilon+2\Omega u=0, \tag{2.2}$$

$$\frac{1}{\rho_0}\frac{\partial p}{\partial x}+\frac{v}{k_x}u-2\Omega v=0, \tag{2.3}$$

$$\frac{1}{\rho_0}\frac{\partial p}{\partial z}-\frac{\rho}{\rho_0}g+\frac{v}{k_z}w=0, \tag{2.4}$$

$$c\frac{\partial T}{\partial t}+v.\nabla T=\kappa_x\frac{\partial^2 T}{\partial x^2}+\kappa_z\frac{\partial^2 T}{\partial z^2}, \tag{2.5}$$

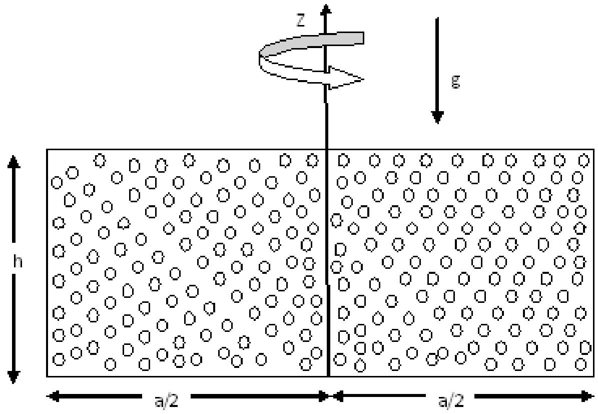

Figure 1. Physical configuration.

$$\frac{\partial S}{\partial t}+u\frac{\partial S}{\partial x}+w\frac{\partial S}{\partial z}=\sigma_x\left(\frac{\partial^2 S}{\partial x^2}+\frac{k_x}{T_m}\frac{\partial^2\theta}{\partial x^2}\right)+\sigma_z\left(\frac{\partial^2 S}{\partial z^2}+\frac{k_z}{T_m}\frac{\partial^2\theta}{\partial z^2}\right) \quad (2.6)$$

$$\rho=\rho_0\ [1-\beta(T-T_0)+\alpha(S-S_0\ )]. \quad (2.7)$$

If T is the absolute temperature, T_0 +T and T_0 are the bottom and top walls temperatures of the box. It is believed that the box's walls will transfer heat and are impermeable. We get Static conduction if fixed temperature circulation does not depend upon x and varies at constant rate on z, based on equations (2.1) to (2.7).

$$T=\left[T_0+\Delta T\left(1-\frac{z}{h}\right)\right]+\theta,$$

$$S=\left[S_0+\Delta S\left(1-\frac{z}{h}\right)\right]+s \quad (2.8)$$

Where θ and s are variations from steady concentration and temperature. As a result of the flow's axis symmetry, Using the stream function, we represent $\psi=\psi(x,y)$ by

$$w=-\frac{\partial\psi}{\partial x},\quad u=\frac{\partial\psi}{\partial z} \quad . \quad (2.9)$$

Asterisks serve as a representation for non-dimensional terms.

$$u=\frac{\kappa_x a u^*}{h^2}, v=\frac{\kappa_y a v^*}{h^2}, w=\frac{\kappa_z w^*}{h}, t=\frac{c h^2 t^*}{\kappa_z};$$

$$\psi=\frac{\kappa_z a\psi^*}{h},\ \theta=\Delta T\theta^*,\ T_0=\Delta T T_0^*,\ p=\frac{v k_z\rho_0 p^*}{k_z},\ S=\Delta S S^* \quad (2.10)$$

The governing equation has the following form when the aforementioned expressions are introduced into equations (2.1)–(2.7):

$$\left(\xi\frac{\partial^2}{\partial x^2}+\frac{\partial^2}{\partial z^2}\right)\psi+\xi R_a\frac{\partial\theta}{\partial x}-\xi R_S\frac{\partial s}{\partial x}-T_a\frac{\partial v}{\partial z}=0, \quad (2.11)$$

$$\chi\frac{\partial v}{\partial z}+T_a\frac{\partial^2\psi}{\partial z^2}=0, \quad (2.12)$$

$$P_c\left(\zeta\frac{\partial^2}{\partial x^2}+\frac{\partial^2}{\partial z^2}\right)s+P_s\left(\zeta_1\frac{\partial^2}{\partial x^2}+\frac{\partial^2}{\partial z^2}\right)\theta-\frac{\partial\psi}{\partial x}=\frac{\partial s}{\partial t} \quad (2.13)$$

$$\left(\eta\frac{\partial^2}{\partial x^2}+\frac{\partial^2}{\partial z^2}\right)\theta-\frac{\partial\psi}{\partial x}=\frac{\partial\theta}{\partial t}. \quad (2.14)$$

The expression for the Rs and Ra the are as follows

$$R_S=\frac{\alpha g k_z\Delta S h}{\upsilon\kappa_z},\qquad R_a=\frac{\beta g k_z\Delta T h}{\upsilon\kappa_z}. \quad (2.15)$$

The equation for the aspect ratio (anisotropy) of temperature diffusivity and permeability are given by the expression

$$\xi=\frac{k_x}{k_z}\left(\frac{h}{a}\right)^2, \zeta=\frac{\sigma_x}{\sigma_z}\left(\frac{h}{a}\right)^2, \eta=\frac{\kappa_x}{\kappa_z}\left(\frac{h}{a}\right)^2, \chi=\frac{k_x}{k_z}.$$

$$P_c=\left(\frac{\sigma_z}{k_z}\right),\ P_s=\left(\frac{\sigma_z}{T_m}\cdot\frac{\Delta T}{\Delta S}\right),\ \zeta_1=\left(\frac{\sigma_x}{\sigma_z}\right)\left(\frac{h}{a}\right)^2\kappa_x \quad (2.16)$$

The BC's for heat-conducting walls are completely impermeable boundaries is provided as

$$S=\psi=\frac{\partial v}{\partial z}=\theta=0 \text{ on}\begin{cases} z=0,\ z=1\ ;\ 0<z<1 \\ x=0.5, x=0.5\ ;-0.5<x<0.5\end{cases} \quad (2.17)$$

3.0 Steady Flow Patterns and Linear Stability

Utilising equations with linearised forms (2.11) to mention free convection (2.14). Solution these equations' in Fourier series can be expressed as

$$\psi=e^{\sigma t}\left[\frac{C_0}{2}+\sum_{n=1}^{\infty}D_n(x)\sin zn\pi+C_n(x)\cos zn\pi\right], \quad (3.1)$$

$$\theta = e^{\sigma t}\left[\frac{F_0}{2} + \sum_{n=1}^{\infty} G_n(x)\sin zn\pi + F_n(x)\cos zn\pi\right], \quad (3.2)$$

$$v = e^{\sigma t}\left[\frac{A_0}{2} + \sum_{n=1}^{\infty} B_n(x)\sin zn\pi + A_n(x)\cos zn\pi\right], \quad (3.3)$$

$$S = e^{\sigma t}\left[\frac{S_0}{2} + \sum_{n=1}^{\infty} S_n(x)\cos zn\pi + H_n(x)\sin zn\pi\right]. \quad (3.4)$$

Where $C_n, D_n, G_n, F_n,, B_n, S_n, H_n$, and A_n are simply expressed in σ. To satisfy the BC's (2.17) .Considering $B_n = C_n = S_n = F_n = 0$ for all x.

By plugging in linearized governing equations, we produce differential equations. (3.1) - (3.4)

$$\left(\xi\frac{d^2}{dx^2} - n^2\pi^2\right)D_n + \xi R_a\frac{dG_n}{dx} - \xi R_S\frac{dH_n}{dx} + T_a n\pi A_n = 0 \quad (3.5)$$

$$\chi A_n + T_a n\pi D_n = 0, \quad (3.6)$$

$$P_c\left(\zeta\frac{d^2}{dx^2} - n^2\pi^2\right)H_n + P_s\left(\zeta_1\frac{d^2}{dx^2} - n^2\pi^2\right)G_n - \frac{dD_n}{dx} = \sigma H_n \quad (3.7)$$

$$\left(\eta\frac{d^2}{dx^2} - n^2\pi^2\right)G_n - \frac{dD_n}{dx} = \sigma G_n. \quad (3.8)$$

And below the BC's for A_n, D_n, G_n and H_n are

$$D_n\left(\frac{1}{2}\right) = D_n\left(-\frac{1}{2}\right) = 0, \qquad A_n\left(\frac{1}{2}\right) = A_n\left(-\frac{1}{2}\right) = 0,$$

$$G_n\left(\frac{1}{2}\right) = G_n\left(-\frac{1}{2}\right) = 0, \qquad H_n\left(\frac{1}{2}\right) = H_n\left(-\frac{1}{2}\right) = 0. \quad (3.9)$$

Therefore, we can substitute σ = 0 in equations (3.7) and (3.8) for the marginal stability and in order to determine (Ra_c) the critical Rayleigh number, is in terms of (ξ, η, ζ, χ) (3.8). smallest eigen value Ra_c is provided by the above group of equations (3.5) to (3.8) along with the boundary conditions (3.9). The typical answer takes the form

$$G_n(x, R_a) = s\left[rC_1\sin px + C_3\sin qx - \left(rC_2\cos px + C_4\cos qx\right)\right] \quad (3.10)$$

$$D_n(x, R_a) = \left[C_1\cos px + C_3\cos qx + C_2\sin px + C_4\sin qx\right] \quad (3.11)$$

$$H_n(x, R_a) = t\left[rC_1\sin px + C_3\sin qx - \left(rC_2\cos px + C_4\cos qx\right)\right] \quad (3.12).$$

$$A_n = \frac{-n\pi T_a}{\xi}\left[C_1\cos p\,x + C_2\sin p\,x + C_3\cos q\,x + C_4\sin q\,x\right] \quad (3.13).$$

C_i's are arbitrary constants

$$p_q = \frac{1}{2\sqrt{\xi}}\left\{\left[\sqrt{R_a - (1-P_s)\frac{R_S}{P_c} - n^2\pi^2\left(2 + \frac{T_a^2}{\xi}\right) + 2n^2\pi^2\sqrt{1 + \frac{T_a^2}{\xi}}}\right] \pm \left[\sqrt{R_a - (1-P_s)\frac{R_S}{P_c} - n^2\pi^2\left(2 + \frac{T_a^2}{\xi}\right) - 2n^2\pi^2\sqrt{1 + \frac{T_a^2}{\xi}}}\right]\right\} \quad (3.14)$$

$$r = \frac{q\left(\xi p^2 + n^2\pi^2\left(1 + \frac{T_a^2}{\xi}\right)\right)}{p\left(\xi q^2 + n^2\pi^2\left(1 + \frac{T_a^2}{\xi}\right)\right)},$$

$$s = \frac{\xi q^2 + n^2\pi^2\left(1 + \frac{T_a^2}{\xi}\right)}{\xi q\left(R_a - (1-P_S)\frac{R_S}{P_c}\right)},$$

$$t = -\frac{1-P_S}{P_C}\left(\frac{\xi q^2 + n^2\pi^2\left(1 + \frac{T_a^2}{\xi}\right)}{\xi q\left(R_a - (1-P_S)\frac{R_S}{P_c}\right)}\right). \quad (3.15)$$

At The boundary requirements at $Ra \neq Ra_c$ guarantee that $p \neq q$, the non-trivial solution is given by,

I. $(1-r)\sin\left(\frac{q+p}{2}\right) + (1+r)\sin\left(\frac{p-q}{2}\right) = 0$ and

$$C_2 = 0 = C_4 \quad (3.16)$$

II. $(1-r)\sin\left(\frac{q+p}{2}\right) - (1+r)\sin\left(\frac{p-q}{2}\right) = 0$ and

$$C_2 = 0 = C_4. \quad (3.17)$$

When it comes to isotropic medium where $\xi = \eta = \zeta = \chi$, anatical solution of the equations gives Ra_c. Ra_c is found numerically in anisotropic case.

- **The isotropic porous media case**: if $\frac{k_x}{k_z} = \frac{\kappa_x}{\kappa_z}$

then conditions $\xi = \eta = \zeta = \chi$ are satisfied , i.e. number of Thermal diffusivity the parallel and perpendicular components are same as permeability have equal amounts of the parallel and perpendicular components.

For cases I and II, the following prerequisites must be met at r=1

for $m = 1, 2, 3, 4.......$

$$p - q = 2m\pi, \qquad (3.18)$$

It gives

$$R_a = (1-P_s)\frac{R_s}{P_c} + n^2\pi^2\left(2+\frac{Ta^2}{\xi}\right) + 4m^2\pi^2\xi + 2n^2\pi^2\sqrt{1+\frac{T_a^2}{\xi}} \qquad (3.19)$$

Where $m = 1, 2, 3, 4.......$ and $n = 1, 2, 3, 4.......$

the minimum feasible value of the critical Rayleigh number Ra

$$Ra_c = (1-P_s)\frac{R_s}{P_c} + \pi^2\left(2+\frac{Ta^2}{\xi}\right) + 4\pi^2 + 2\pi^2\sqrt{1+T_a^2} \quad .(3.20)$$

The smallest eigen value for an isotropic medium relates to $n = 1$ and $m = 1$

$$Ra_c = (1-P_S)\frac{R_S}{P_C} + \pi^2\left(2+T_a^2\left(\frac{a}{h}\right)^2\right) + 4\pi^2\left(\frac{h}{a}\right)^2 + 2\pi^2\sqrt{1+T_a^2\left(\frac{a}{h}\right)^2} \qquad (3.21)$$

$T_a \to 0$ and $\left(\frac{h}{a}\right) \to 0$ the channel go toward an infinitesimally thin layer of porous material. In this situation, the critical Rayleigh number $Ra_c = 4\pi^2$ coincides with a permeable layers conclusion that is commonly accepted Boris[17]. Critical value calculated using the equation (3.21), however, differs from the conclusion reached by Sutton[18] for a channel with completely insulating walls. The solution of equation (3.21) $Ra_c = 8\pi^2$ for a square box $h = a$, or one with fully insulating lateral walls, is while the result for a rectangular box is $Ra_c = 4\pi^2$. Because of the heat diffusion over the walls in this instance. Conducting a lateral wall box is anticipated to result in a higher critical value.

The fluid flow at the start of natural convection corresponds to a moderately supercritical Rayleigh number. Due to the fact that the conditions in equations (3.16) and (3.17) coincide. There are two independent answers to the BVP. Additionally, equations (2.11) and show this (2.14).

At $Ra = Ra_c$, let ψ_0, θ_0, S_0,and v_0, are the solutions , then the solutions are

$\psi_1 = -\xi\theta_0 R_a$, $v_1 = v_0$ and $\theta_1 = \psi_0$ linearly independent.

The solution are provided as

Table 1. Ra_c as various combinations of ξ and η. Isotropic cased is represented in the principle diagonal

ξ/η	0.125	0.25	0.5	1	2	4	8
0.125	197551	69842	13035	3078	3154	1158	377
0.25	279388	98780	25676	6171	4439	1616	542
0.5	395126	139708	50789	12357	6258	2266	779
1	558811	197595	100775	24728	8837	3191	1119
2	790307	279471	200409	49471	12496	4511	1612
4	1117716	395284	399196	98958	17693	6401	2333
8	1580788	559115	796093	197931	25090	9121	3398

$$\theta^{(1)} = Qs\sin Kx\cdot\sin\pi x\cdot\sin z\pi \;;$$

$$\psi^{(1)} = Q\cos Kx\cdot\sin\pi z\cdot\sin\pi x$$

$$s^{(1)} = -Q\sin Kx\sin\pi x\sin\pi z \qquad (3.22)$$

$$\theta^{(2)} = S\sin Kx\cdot\cos\pi z\cdot\sin\pi x \;;$$

$$\psi^{(2)} = \frac{S}{s}\cos Kx\cdot\sin\pi z\cdot\sin x\pi$$

$$s^{(2)} = -\frac{T_a\pi S}{s\xi}\cos Kx\cdot\sin\pi z\cdot\cos\pi x\,;$$

$$v^{(2)} = -\frac{St}{s}\sin Kx\cdot\cos\pi z\cdot\cos\pi x \qquad (3.23)$$

where and are the amplitude Q and Sconstants. Equation (3.22) gives a symmetric flow pattern with total number of cells 2n, here the cell count varies based on ξ. The following equation gives a symmetric flow configuration with total number of cells 2n±1 cells (3.23).

ii. The Anisotropic case:

Here, $\xi \neq \eta = \zeta \neq \chi$ The requirement of the non-trivial solutions for above satisfied is . Solution is in the form of

For case i).

$$G_n(x) = -s\left[r\cos(px) - \frac{\sin\left(\frac{p}{2}\right)}{\sin\left(\frac{q}{2}\right)}\cos(qx)\right],$$

$$D_n(x) = \left[\sin(px) - \frac{\sin\left(\frac{p}{2}\right)}{\sin\left(\frac{q}{2}\right)}\sin(qx)\right],$$

$$H_n(x) = -t\left[r\cos(px) - \frac{\sin\left(\frac{p}{2}\right)}{\sin\left(\frac{q}{2}\right)}\cos(qx)\right],$$

$$A_n(x) = \frac{-n\pi T_a}{\chi}\left[\sin(px) - \frac{\sin\left(\frac{p}{2}\right)}{\sin\left(\frac{q}{2}\right)}\sin(qx)\right].$$

and for case ii).

$$G_n(x) = -s\left[r\sin(px) - \frac{\cos\left(\frac{p}{2}\right)}{\cos\left(\frac{q}{2}\right)}\sin(qx)\right],$$

$$D_n(x) = \left[\cos(px) - \frac{\cos\left(\frac{p}{2}\right)}{\cos\left(\frac{q}{2}\right)}\cos(qx)\right],$$

$$A_n = \frac{-n\pi T_a}{\chi}\left[\cos(px) - \frac{\cos\left(\frac{p}{2}\right)}{\cos\left(\frac{q}{2}\right)}\cos(qx)\right],$$

$$H_n(x) = t\left[r\sin(px) - \frac{\cos\left(\frac{p}{2}\right)}{\cos\left(\frac{q}{2}\right)}\sin(qx)\right].$$

Numerous eigenvalues are defined for solutions (i) and (ii). In each of the aforementioned cases, let there be two least eigenvalues Ra_1 and Ra_2.

These values are present at $n=1$. For a given value of ξ, η, ζ and χ, Ra_1 and Ra_2 are computed using form equations (3.16) and (3.17). Critical Rayleigh number $Ra_c=\{Ra_1$and $Ra_2\}$, normally are unequal, which indicates that the values for Ra_1 and Ra_2 are exclusive.

4.0 Conclusion

In the present experiment, natural convection in a three-dimensional cavity is reduced to two-dimensional double diffusive convection with components that diffuse solute and temperature in isotropic and asisotropic porous media in order to examine the impact of uneven temperature changes on natural convection in a three-dimensional rectangular cavity.

It is believed that a rectangular hollow is both heat-conductive and impermeable. The rectangular cavity is heated unevenly from bottom after the addition of solutes to produce temperature distributions and linear concentration pointing in opposite directions.

- Significant wall heating suggests non-dimensional characteristics Because Darcy-Prandtl values are

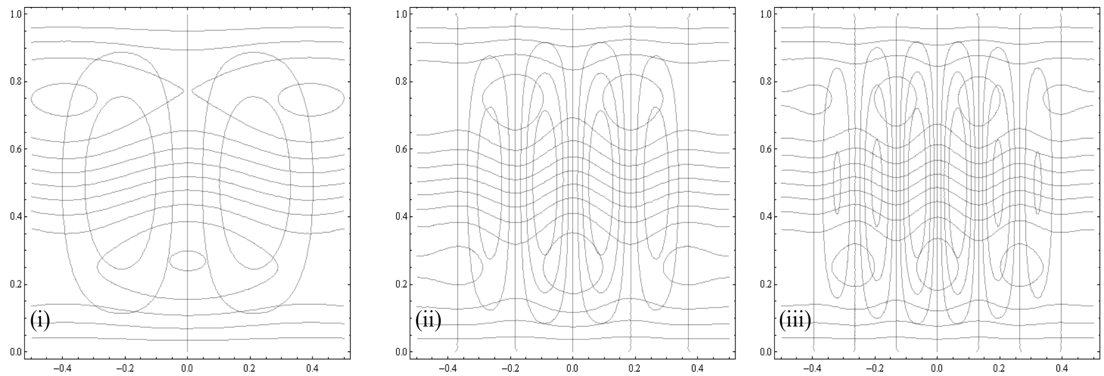

Figure 2. Flow pattern (Stream lines) and Isothermal lines in isotropic case (T_a-varying).

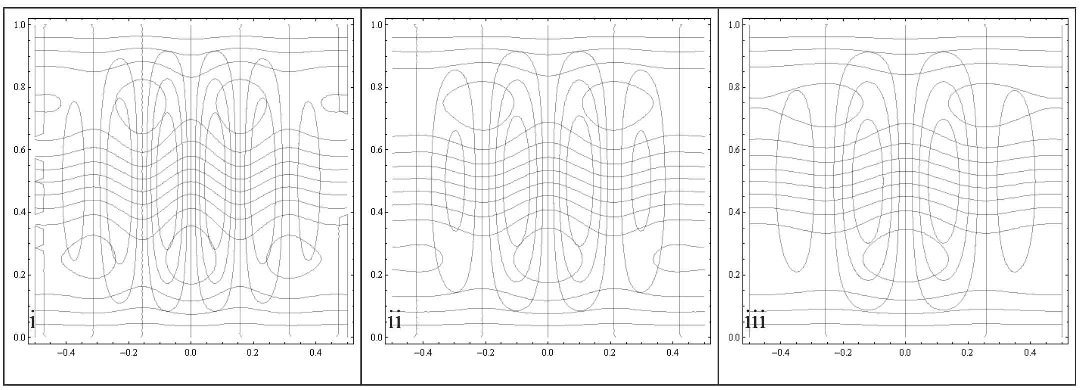

Figure 3. Flow pattern (Stream lines) and Isothermal lines in isotropic case (ξ varying).

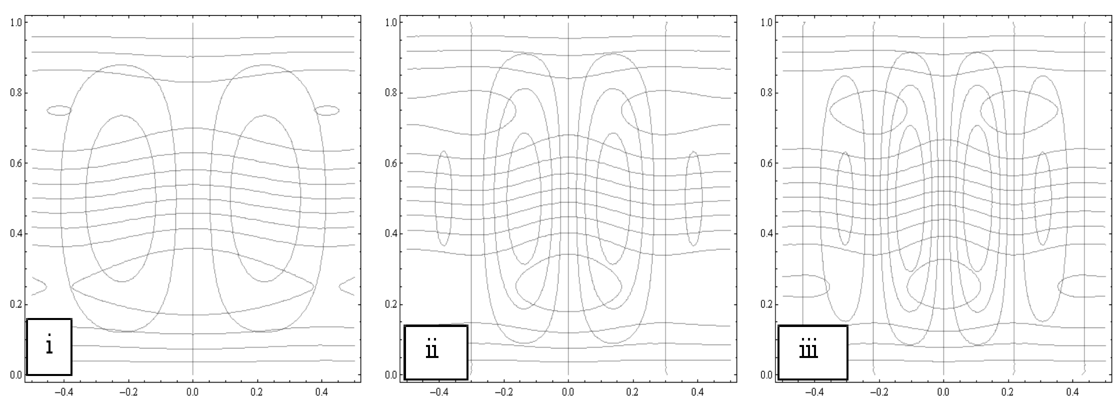

Figure 4. Flow pattern (Stream lines) and Isothermal lines in anisotropic case (T_a-varying).

large, the inertial and viscous components of the momentum equation are disregarded.

- The stream function, as the flow Y – axis symmetric, linear stability theory is applied to find the solutal Ra and critical Ra number.

The associated anisotropic eigen value issue, whose eigen value is to be calculated, and the critical Rayleigh number Ra_c that results from its solution in the form

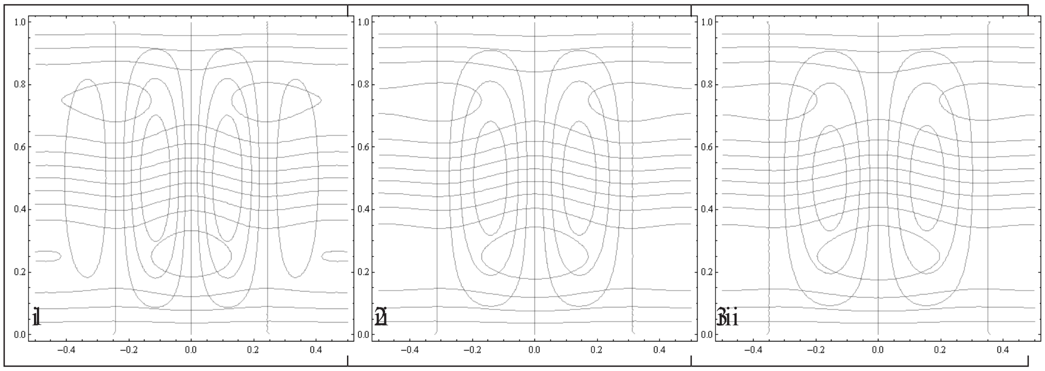

Figure 5. Flow pattern (Stream lines) and Isothermal lines in anisotropic case (ξ-varying).

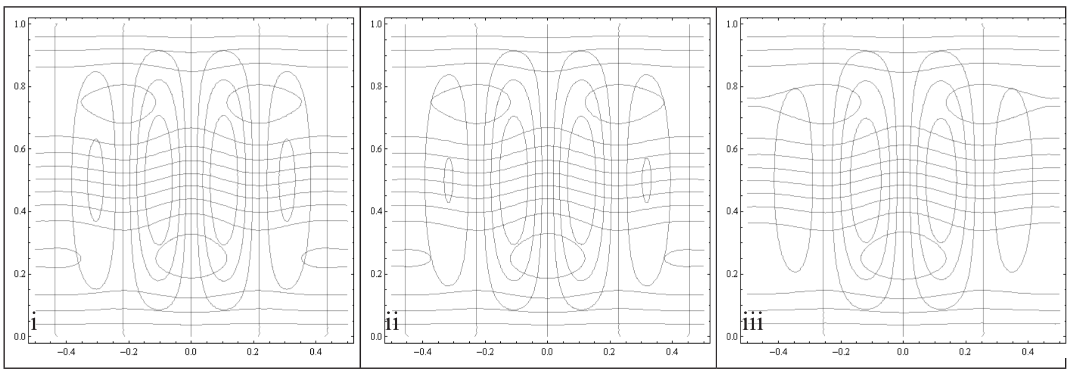

Figure 6. Flow pattern (Stream lines) and Isothermal lines in anisotropic case (χ-varying).

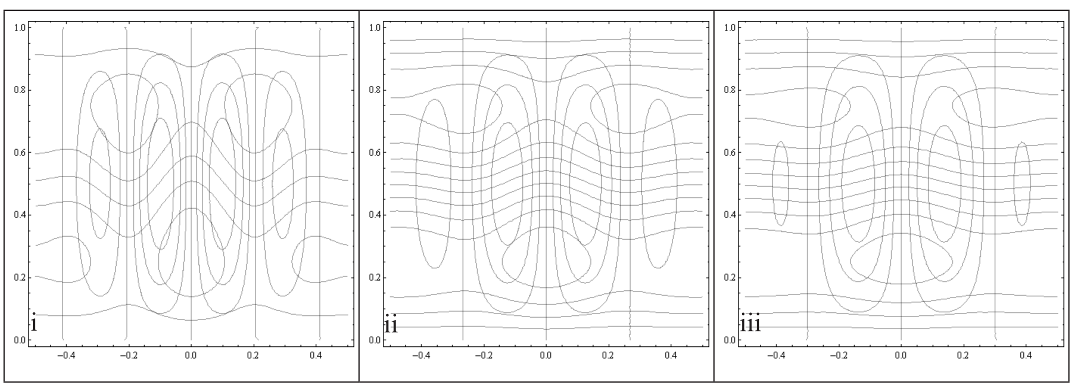

Figure 7. Flow pattern (Stream lines) and Isothermal lines in anisotropic case (η-varying).

$$Ra_C = 4\pi^2\left[\eta + \left(1 + \sqrt{\frac{\eta}{\xi}\left(1 + \frac{T_a^{\ 2}}{\chi}\right)}\right)^2\right] + (1 - P_S)\frac{R_S}{P_c}.$$

$$Ra_c = 4\pi^2\left[\xi + \frac{1}{2}\left(1 + \frac{T_a^{\ 2}}{2\xi} + \sqrt{\left(1 + \frac{T_a^{\ 2}}{\xi}\right)}\right)\right] + (1 - P_S)\frac{R_S}{P_c}$$

The output is consistent with the earlier outputs when Taylor's number is zero, it reduces to the Rayleigh number discovered in the non-rotating case, when Taylor's number is zero in the isotropic case, as the ristriction $\frac{h}{a} \to 0$ it simplifies to the standard form $Ra_c = R_S + 4\pi^2$ and $Ra_c = 4\pi^2$, and when $R_S = 0$, double duffusing component is absent, which is consistent with [11] the

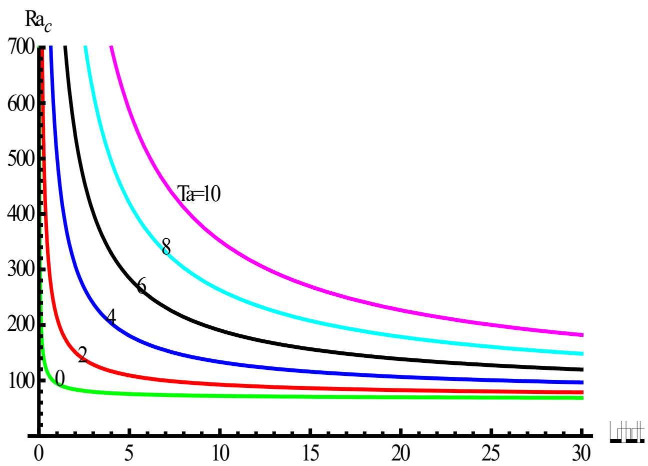

Figure 8. Plot between Ra_c and ξ/η (ξ=0.5, Rs=50, η=0.125).

most commonly accepted porous layers result. At moderately supercritical Rayleigh numbers, two sets of linearly independent solutions are derived, each of which displays a different nice steady flow pattern.

Plotting the critical Ra against the permeability to thermal diffusivity ratio is shown in Figure 8. The finding demonstrates that the relationship between the (Rac) critical Rayleigh number and the ratio ξ / η is inverse. Rotation has the consequence of making the system more unstable since the Solutal Rayleigh number keeps increasing along with the growing Taylors number.

The streamlines' and isothermal lines' flow patterns:

- For both isotropic and anisotropic situations, it was discovered that the number of cells rose as the Taylor's number rose, Figures 2 and 4. The coriolis force increases along with Taylor's number which increases the total number of revolutions. The streamlines and isothermal lines grow as rotation increases. The isothermal lines demonstrate how rotation in an anisotropic system affects oscillatory flow pattern (Figure 7).
- With increasing anisotropy in the anisotropic case, isotherm lines get flatter (Figures 5 and 6). It was discovered that the number of cells reduced as aspect ratio and thermal diffusivity increased.

5.0 References

1. Nield DA, Bejan A. Convection in Porous Media, second ed. Springer Verlag, New York. 1999. https://link.springer.com/book/10.1007/978-1-4614-5541-7
2. Pop I, Ingham DB. Convection Heat Transfer: Mathematical and Computational Modelling of Viscous Fluid and Porous Media, Pergamon, Oxford, 2001.
3. Eckeret ERG, Drake RM. Analysis of Heat and Mass Transfer", McGraw Hill, New York. 1972.
4. Rudriah N, Patil PR. 5th Intl. Conf. Heat Transfer, Tokyo, CT 3-l 79. 1974.
5. Anghel M, Takhar HS, Pop I. Dufour and Soret Effects on free convection boundary-layer flow over a vertical surface embedded in a porous medium, Studia Universitatics Babes-Bolyai, Mathematica, XLV 11–23. 2000.
6. Postelnicu A. Influence of magnetic field on heat and mass transfer from vertical surfaces in porous media considering Soret and Dufour effects. Int. J. Heat Mass Transfer. 2004; 47:1467–72. https://doi.org/10.1016/j.ijheatmasstransfer.2003.09.017
7. Partha MK, Murthy PVSN, Raja Sekhar GP. Soret and Dufour effects in a non-darcy porous medium. Journal of Heat Transfer. 2006; 128:605-10. https://doi.org/10.1115/1.2188512
8. Lakshmi Narayana PA, Murthy PVSN. Soret and Dufour effects on free convection heat and mass transfer from a horizontal flat plate in a Darcy porous medium. Journal of Heat Transfer. 2008; 130:104504-1–104504-5. https://doi.org/10.1115/1.2789716
9. Mansour A, Amahmid A, Hasnaoui M, Bourich M. Multiplicity of solutions induced by thermosolutal convection in a square porous cavity heated from below and submitted to horizontal concentration gradient in the presence of Soret effect. Numerical Heat Transfer. 2006; Part A 49 69–94.https://doi.org/10.1080/10407780500302166
10. Lakshmi Narayana PA, Murthy PVSN. Soret and Dufour effects in a doubly stratified Darcy porous medium. Journal of Porous Media. 2007; 10:613–24. https://doi.org/10.1615/JPorMedia.v10.i6.70
11. Anjali Devi SP, Kandasamy R. Effects Of chemical reaction, heat and mass transfer on non-linear MHD laminar boundary-layer flow over a wedge with suction or injection. Int. Communication in Heat Mass Transfer. 2002; 29(5):707-16. https://doi.org/10.1016/S0735-1933(02)00389-5
12. Dursunkaya Z, Worek WM. Diffusion-thermo and thermal diffusion effects in transient and steady natural convection from a vertical surface. Int. J. Heat Mass Transfer. 1992; 35:2060-5. https://doi.org/10.1016/0017-9310(92)90208-A

13. Alam MS, Rahman MM. Dufour and Soret effects on mixed convection flow past a vertical porous flat plate with variable suction. Nonlinear Analysis: Modelling and Control. 2006; 11(6):3-12. https://www.researchgate.net/publication/252626188_Dufour_and_Soret_effects_on_mixed_convection_flow_past_a_vertical_porous_plate_with_variable_suction https://doi.org/10.15388/NA.2006.11.1.14761
14. Srinivasacharya D, Ch RamReddy. Soret and Dufour Effects on mixed convection in a non-darcy micropolar fluid. Int. J of non – linear science. 2010; 11(2):246-55.
15. Malashetty MS, Gaikwad SN, Swamy M. An analytical study of linear and non-linear double diffusive convection with Soret effect in couple stress liquids. Int. J Therm. Sci. 2006; 45:897-907. https://doi.org/10.1016/j.ijthermalsci.2005.12.005
16. A. Tilgner. Rotational Dynamics of the Core. Treatise on Geophysics. 2015; 8:183–212.https://doi.org/10.1016/B978-0-444-53802-4.00140-8
17. Bories S, Natural Convection in porous media. Advances in Transport Phenomena in Porous Media, NATO ASI Series book series. 1987; 128:77-141. https://link.springer.com/chapter/10.1007/978-94-009-3625-6_4 https://doi.org/10.1007/978-94-009-3625-6_4
18. Sutton FM. Onset of convection in a porous channel with net through flow. Physics of Fluids. 1970; 13(8):1931. https://doi.org/10.1063/1.1693188

Nomenclature

$\beta =$ Thermal expansion co-efficient	$\vec{q} = (u, v, w) =$ fluid velocity	$s =$ Deviation from the static concentration
$h =$ Rectangular channel height	$R_a =$ Rayleigh Number (Thermal)	$\Delta S =$ Characteristic Concentration difference
$a =$ rectangular channel width	$T =$ Temperature	$S_0 =$ Reference Concentration
$c =$ Specific heat at constant pressure	$\Delta T =$ Characteristic temperature difference	$\sigma =$ Growth rate
$\kappa = (\kappa_x, \kappa_y, \kappa_z)$ Thermal diffusivity in anisotropic porous media along x, y, z axis	$t =$ Time	$\xi = \frac{k_x}{k_z}\left(\frac{h}{a}\right)^2 =$ Anisotropic ratio
$\kappa =$ Thermal diffusivity in isotropic case	$\theta =$ Static temperature deviation	$T_a = \frac{2\Omega d^2}{\nu} =$ Taylors Number
$k =$ In isotropic case Permeability	$\vec{g} = (0, 0, -g)$ acceleration due to gravity	$\Omega = (0, 0, \Omega) =$ system fixed angular velocity
$k = \left(k_x, k_y, k_z\right)$ Permeability along coordinate axes in anisotropic porous media	$T_0 =$ Reference temperature	$\eta = \frac{\kappa_x}{\kappa_z}\left(\frac{h}{a}\right)^2 =$ Aspect ratio
$p_1 =$ Pressure	$\rho_0 =$ Reference density	$\nabla = \left(\frac{\partial}{\partial x}, \frac{\partial}{\partial y}, \frac{\partial}{\partial z}\right) =$ Three dimensional gradient operator
$p = p_1 - \frac{1}{2}\lvert\Omega \times r\rvert$	$\left(\rho c_v\right)_S, \left(\rho c_v\right)_f =$ Heat capacity per unit volume of the solid and fluid	$\nabla^2 = \left(\frac{\partial^2}{\partial x^2}, \frac{\partial^2}{\partial y^2}, \frac{\partial^2}{\partial z^2}\right) =$ Laplacian operator
	$\rho =$ Density	
	$\nu =$ Thermal viscosity	
	$\psi = \psi\left(x, y\right) =$ Streamline function	
	$R_c =$ Solutal Rayleigh Number	
	$S =$ Concentration	